Bioorganic & Medicinal Chemistry Letters xxx (2016) xxx–xxx

Contents lists available at ScienceDirect

Bioorganic & Medicinal Chemistry Letters

journal homepage: www.elsevier.com/locate/bmcl

Optimisation of a 5-[3-phenyl-(2-cyclic-ether)-methyl-ether]-4-aminopyrrolopyrimidine series of IGF-1R inhibitors

Robin A. Fairhurst [a,*], Thomas H. Marsilje [b], Stefan Stutz [a], Andreas Boos [a], Michel Niklaus [a], Bei Chen [b], Songchun Jiang [b], Wenshuo Lu [b], Pascal Furet [a], Clive McCarthy [a], Frédéric Stauffer [a], Vito Guagnano [a], Andrea Vaupel [a], Pierre-Yves Michellys [b], Christian Schnell [a], Sébastien Jeay [a]

[a] Novartis Institutes for BioMedical Research, CH-4002 Basel, Switzerland
[b] Genomics Institute of the Novartis Research Foundation, 10675 John Jay Hopkins Drive, San Diego, CA 92121, USA

ARTICLE INFO

Article history:
Received 21 January 2016
Revised 22 February 2016
Accepted 24 February 2016
Available online xxxx

Keywords:
Oncology
Kinase inhibitor
Insulin-like growth factor receptor-1

ABSTRACT

Taking the pyrrolopyrimidine derived IGF-1R inhibitor NVP-AEW541 as the starting point, the benzyl ether back-pocket binding moiety was replaced with a series of 2-cyclic ether methyl ethers leading to the identification of novel achiral [2.2.1]-bicyclic ether methyl ether containing analogues with improved IGF-1R activities and kinase selectivities. Further exploration of the series, including a fluorine scan of the 5-phenyl substituent, and optimisation of the sugar-pocket binding moiety identified compound **33** containing (*S*)-2-tetrahydrofuran methyl ether 6-fluorophenyl ether back-pocket, and *cis*-*N*-Ac-Pip sugar-pocket binding groups. Compound **33** showed improved selectivity and pharmacokinetics compared to NVP-AEW541, and produced comparable in vivo efficacy to linsitinib in inhibiting the growth of an IGF-1R dependent tumour xenograft model in the mouse.

© 2016 Elsevier Ltd. All rights reserved.

The IGF-1/insulin family of growth factors is an evolutionally conserved system which plays a crucial role in the growth and development of many tissues and in the regulation of metabolism. This system comprises three receptors of the receptor tyrosine kinase family: the insulin-like growth factor-1 receptor (IGF-1R); the insulin receptor (InsR) and the IGF-2/mannose 6-phosphate receptor (M-6-PR). These receptors interact with three ligands (insulin, IGF-1, and IGF-2), which also interact with six known types of circulating IGF-binding proteins (IGFBP1–6).[1] The IGF-1R is widely expressed in many human tissues and cell types and is highly homologous to the InsR. However, these two receptors have distinct functions, since the IGF-1R controls apoptosis, cell growth, and differentiation, while the InsR regulates primarily physiological processes. Additionally, the ability of the highly homologous IGF-1R and InsR to form hybrid receptors through hetero dimerization further increases the complexity of the signalling system.[2]

Mitogenic activity of IGF-1 was first established in breast carcinoma and the anti-tumour activity of an IGF-1R specific antibody was first demonstrated now over a quarter of a century ago.[3] Since then, substantial population and preclinical data have all pointed towards the IGF-1R pathway as an important regulator of tumour cell biology, and as a result many groups have identified antibody and low molecular weight inhibitors which have entered into multiple clinical studies exploring the safety and anti-tumour activity of these agents. Although the results of these clinical trials have been mixed, in particular when tested as a single agent, a growing effort is indicating the potential for inhibiting the IGF-1R pathway in combination with cytotoxic chemotherapy and various targeted agents.[4] Therefore, assessing optimal combination therapies could represent new opportunities for the development of IGF-1R inhibitors in a range of common cancer indications.

Of the numerous IGF-1R inhibitors that have been developed since the link to cancer was established those targeting the kinase activity, through binding within the adenosine triphosphate (ATP) binding site, represent the most common approach taken.[5] Of these linsitinib is the most advanced compound which is currently in multiple phase II studies, in a range of cancers, in combination with other treatment modalities.[6] Prior to the disclosure of linsitinib workers at Novartis had described the identification of the structurally related 5-phenyl-4-aminopyrrolopyrimidine derivative NVP-AEW541, Figure 1.[7] This molecule has subsequently been used extensively as an IGF-1R inhibitor tool compound in a number of preclinical investigations.[8] In this letter we describe the further optimisation of the 5-phenyl-4-aminopyrrolopyrimidine series, to improve upon NVP-AEW541, utilising the observation

* Corresponding author at present address: Novartis Institutes for Biomedical Research, Global Discovery Chemistry, Novartis Pharma AG, Werk Klybeck, Postfach, CH-4002 Basel, Switzerland. Tel.: +41 61 6964294; fax: +41 61 6966246.
E-mail address: robin.fairhurst@novartis.com (R.A. Fairhurst).

http://dx.doi.org/10.1016/j.bmcl.2016.02.075
0960-894X/© 2016 Elsevier Ltd. All rights reserved.

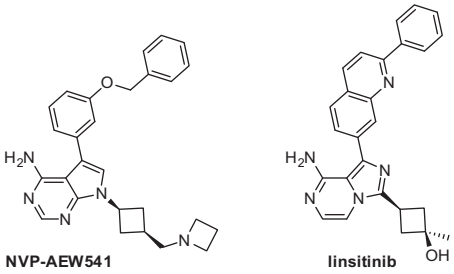

Figure 1. Structures of NVP-AEW541 and linsitinib.

described in the preceding letter that 2-cyclic ether methyl ethers can be used to replace the benzyl ether moiety.[9]

The switch to a 2-cyclic ether methyl ether sub-series, as exemplified by the 2-tetrahydrofuran (THF) analogue **1** shown in Figure 2, was envisioned as an opportunity to improve upon a number of the limitations that had been identified for the benzyl ether NVP-AEW541: cyclic ethers were anticipated to provide an increase in aqueous solubility and enable an adequate level of solubility to be achieved without the need for a strongly basic group, helping to reduce the cardiovascular risk associated with inhibition of the human ether-à-go-go related gene (hERG) channel; in vitro and in vivo metabolism studies indicated greatly reduced cleavage of the aryl ether for the cyclic ethers,[9,10] minimising the formation of the phenol **2**, which has been shown to be a multi-targeted kinase inhibitor.[11,12] Therefore, although NVP-AEW541 provided satisfactory exposure to deliver efficacy in rodent xenograft models and also showed a good kinase selectivity profile,[7] at the onset of the optimisation the 2-cyclic ether methyl ether sub-series was seen as an opportunity to identify 5-phenyl-4-aminopyrrolopyrimidine analogues with improved pharmacokinetic (PK) and tolerability/safety profiles.

To explore the 2-cyclic ether methyl ether structure activity relationship (SAR) further, the observation that both enantiomers of the 2-THF methyl ether showed similar high levels of activity attracted our attention.[9] In particular, for each enantiomer, modelling indicated the cyclic ether oxygen atom makes the same hydrogen bond with Lys1033. As a result, the remaining atoms of each THF ring of the two enantiomers are positioned within the IFG-1R ATP-pocket in orientations which suggested a 7-oxabicyclo[2.2.1]heptan-1-ylmethylether could be accommodated. Such an achiral [2.2.1]-bicyclic ether moiety would then be postulated to simultaneously make the hydrophobic contacts associated with both 2-THF methyl ether enantiomers within the back-pocket region. In addition to the potential for increasing potency, the further filling of the relatively large back-pocket region of the IGF-1R ATP binding site was anticipated to further improve the, already high, kinase selectivity for the series.[12] To explore this possibility compound **3**, the direct analogue of NVP-AEW541, was targeted for synthesis and the structure is shown in Figure 3. Modelling supported the above hypothesis with the [2.2.1]-bicyclic ether making hydrophobic contacts with residues Met1054, Phe1154, Phe1047,

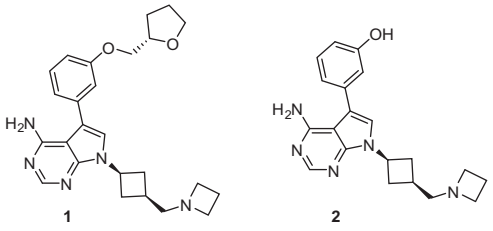

Figure 2. Structures of the (*S*)-tetrahdrofuran-2-yl methyl ether analogue **1** and the metabolite **2** formed upon cleavage of the phenyl ether.

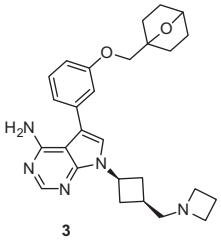

Figure 3. Structure of the 7-oxabicyclo[2.2.1]heptan-1-ylmethyl ether analogue **3**.

Phe1010 and Glu1050 in addition to the hydrogen bond with Lys1033. Compound **3** docked into ATP-site of IGF-1R is shown in Figure 4, and the model is based upon the X-ray structure of a cyclic ether analogues with the closely related InsR (PDB code: 5HHW).[9]

To prepare analogues containing the 7-oxabicyclo[2.2.1]heptan-1-ylmethylether moiety the convergent approach outlined in Schemes 1 and 2 was developed in which the 5-phenyl pyrrolopyrimidine substituent was introduced via a Suzuki reaction in the final phase of the synthesis.[13] Preparation of the phenyl coupling partner is shown in Scheme 1 and started from the mono-ketal of cyclohexane-1,4-dione **4** which gave the vinyl alcohol **5** following a sequence of methylenation, ketal deprotection and reduction. Cyclisation of **5** through activation of the double bond with iodine provided the iodide **6** which was then used to alkylate the phenol leading to the key building block **7**.

Scheme 2 shows the synthesis and reaction of the pyrrolopyrimidine coupling partner which starts with the annulation of 2-(4,6-dichloropyrimidin-5-yl)acetaldehyde **8** upon reaction with the benzoyl ester of *cis*-4-hydroxymethyl cyclobutylamine **9**[14] to give the pyrrolopyrimidine **10**. Iodination of **10** produced the 5-iodo analogue and subsequent displacement of the 4-chloro substituent with ammonia yielded **11** which readily underwent a Suzuki reaction with **7** to give compound **12** with the key pharmacophore elements in place. Manipulation of the hydroxymethylcyclobutyl pyrrolopyrimidine 7-substituent via periodinane oxidation followed by a reductive amination with the newly formed aldehyde generated the targeted compound **3**.

The IGF-1R activities of the compounds were measured using a biochemical assay and with cellular assays measuring p-IGF-1R in HEK cells and IGF-1R dependent proliferation in Ba/F3 cells, data are shown in Table 1.[15] In line with the binding hypothesis, the [2.2.1] bicyclic ether analogue **3** was found to be well tolerated

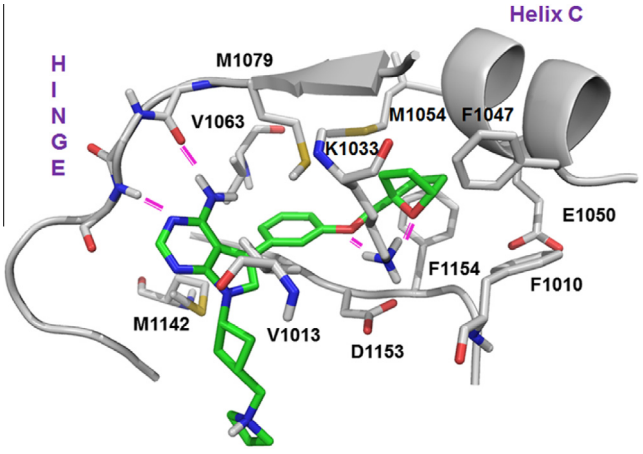

Figure 4. Model of compound **3** docked into the ATP site of IGF-1R. Key hydrogen-bonds are indicated with magenta lines: pyrrolopyrimidine N5 to M1082 NH 3.2 Å, pyrrolopyrimidine 4-NH to E1080 C=O 2.9 Å, aryl ether to K1033 side-chain NH 3.0 Å, [2.2.1] bicyclic ether to K1033 side-chain NH 2.8 Å.

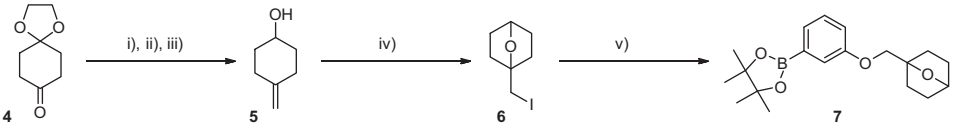

Scheme 1. Synthesis of the 7-oxabicyclo[2.2.1]heptan-1-ylmethyl ether intermediate **7**. Reagents and conditions: (i) methyltriphenylphosphonium bromide, *n*-BuLi, THF, −10 to 25 °C, 17 h (92%); (ii) $(CO_2H)_2$, acetone, H_2O, 25 °C, 3.5 h (87%); (iii) $NaBH_4$, THF, 3 h, 25 °C (100%); (iv) 2.5 equiv I_2, Na_2CO_3, AcCN, 22 h, 25 °C (42%); (v) 3-hydroxyphenyl boronic acid pinacol ester, NaH, $Et_4N^+I^-$, DMF, 100 °C, 6 h (66%).

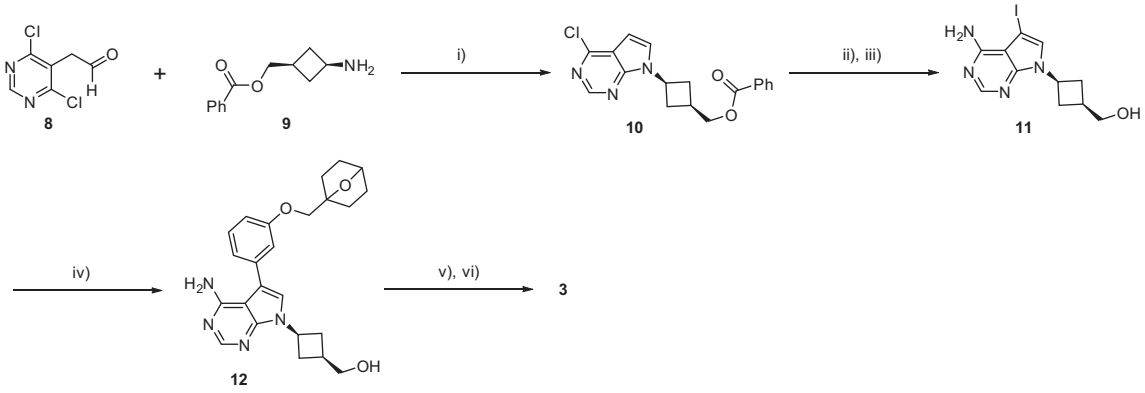

Scheme 2. Synthesis of the 7-oxabicyclo[2.2.1]heptan-1-ylmethyl ether containing analogues **12** and **3**. Reagents and conditions: (i) Hünig's base, EtOH, 6 h, 80 °C (67%); (ii) *N*-iodosuccinimide (NIS), DMF, 23 h, 25 °C (92%); (iii) NH_4OH, dioxane, 23 h, 110 °C (58%); (iv) **7**, $(Ph_3P)_4Pd$, Na_2CO_3, H_2O, DMF, 16 h, 80 °C (80%); (v) 2-iodoxybenzoic acid, AcCN, 1 h, 80 °C (25%); (vi) azetidine, $Na(OAc)_3BH$, AcOH, 1,2-DCE, 25 °C, 1 h, then reversed-phase chromatography (22%).

within the ATP-binding site and led to a similar level of IGF-1R activity compared to NVP-AEW541 and the (*S*)-2-THF analogue **1** at both the biochemical and cellular level. However, there is an overall trend in Table 1 for the [2.2.1] bicyclic ethers to be slightly more potent compared to the (*S*)-2-THF analogues, vide infra, supporting the original hypothesis of increasing favourable interactions within the ATP site of IGF-1R. From the initial study the most potent THF analogues incorporated 5,5-dimethyl substitution in the THF moiety,[9] and to explore this possibility in the [2.2.1] bicyclic ether series the 4-methyl analogue of **12**, compound **13**, was prepared as outlined in Scheme 3. Following an analogous approach to the sequence shown in Scheme 1, but replacing the ketone reduction step by a methyl Grignard addition, the key intermediate **14** was readily prepared and converted to the boronate ester **15** in 3 steps. Suzuki coupling between **15** and **11** then gave the targeted compound **13**.

Comparison of the IGF-1R activity of **13** with **12** indicated no increase in IGF-1R activity upon the introduction of the 4-methyl group into the 7-oxabicyclo[2.2.1]heptan-1-ylmethyl ether moiety in contrast to the SAR seen for the 2-THF analogues. With no added benefit from the 4-methyl group these analogues were not pursued further.

Table 1
Biochemical and cellular IGF-1R activities for the cyclic ether analogues, the phenol **2** and the reference compounds NVP-AEW541 and linsitinib

Compound	Ether moiety	Phenyl substituent	Cyclobutyl 3-substituent	IGF-1R IC_{50} (nM)	HEK IC_{50} (nM)	Ba/F3 IC_{50} (nM)
NVP-AEW541	Bn	H	*cis*-CH_2-azetidine	61	65	20
Linsitinib	See Figure 1		*trans*-Me-*cis*-OH	14	2.8	7.6
1	(*S*)-2-THF-CH_2	H	*cis*-CH_2-azetidine	84	n.d.	12
2	H	H	*cis*-CH_2-azetidine	420	n.d.	454
3	[2.2.1]-CH_2	H	*cis*-CH_2-azetidine	46	53	14
12	[2.2.1]-CH_2	H	*cis*-CH_2OH	33	128	11
13	4-Me-[2.2.1]-CH_2	H	*cis*-CH_2OH	47	183	29
16	[2.2.1]-CH_2	H	*cis*-CH_2-TMSO	n.d.	64	21
17	[2.2.1]-CH_2	H	*cis*-*N*-Ac-Pip	9.4	10	16
25	(*S*)-2-THF-CH_2	H	*cis*-CH_2-TMSO	80	232	92
26	[2.2.1]-CH_2	2-F	*cis*-CH_2-TMSO	4.3	n.d.	n.d.
27	[2.2.1]-CH_2	2-F	*cis*-*N*-Ac-Pip	9.6	2.8	<4.6
28	(*S*)-2-THF-CH_2	2-F	*cis*-*N*-Ac-Pip	16	16	15
29	[2.2.1]-CH_2	6-F	*cis*-CH_2-TMSO	8.3	8.9	7.3
30	(*S*)-2-THF-CH_2	6-F	*cis*-CH_2-TMSO	16	14	27
31	(*R*,*S*)-2-Oxetanyl-CH_2	6-F	*cis*-CH_2-TMSO	200	n.d.	251
32	[2.2.1]-CH_2	6-F	*cis*-*N*-Ac-Pip	13	12	7.8
33	(*S*)-2-THF-CH_2	6-F	*cis*-*N*-Ac-Pip	12	13	16
34	(*R*)-2-THF-CH_2	6-F	*cis*-*N*-Ac-Pip	64	159	47
35	(*S*)-2-THF-CH_2	6-F	*trans*-*N*-Ac-Pip	54	n.d.	n.d.
36	(*S*)-2-THF-CH_2	5-F	*cis*-CH_2-TMSO	260	1291	n.d.
37	(*R*)-2-THF-CH_2	5-F	*cis*-CH_2-TMSO	1100	5602	n.d.
38	[2.2.1]-CH_2	4-F	*cis*-CH_2-TMSO	12	31	n.d.

n.d. not determined.

Please cite this article in press as: Fairhurst, R. A.; et al. *Bioorg. Med. Chem. Lett.* (2016), http://dx.doi.org/10.1016/j.bmcl.2016.02.075

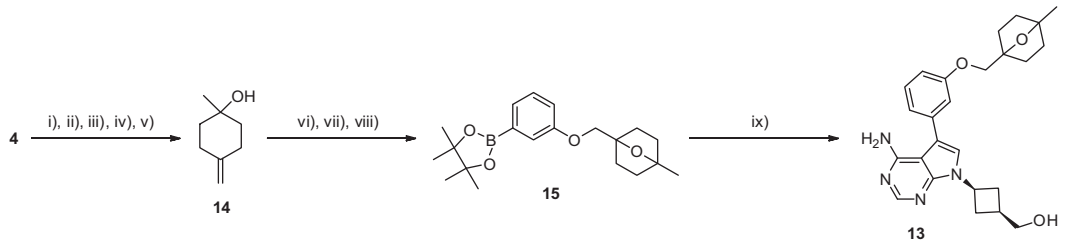

Scheme 3. Synthesis of the 4-methyl-7-oxabicyclo[2.2.1]heptan-1-ylmethyl ether containing analogue **13**. Reagents and conditions: (i) slow addition MeMgBr, Et_2O, 25 °C (85%); (ii) 1 N $HCl_{(aq)}$, 25 °C, 24 h (87%); (iii) 3,4-dihydro-2H-pyran, cat. *p*TSA, 25 °C with cooling, 45 min (81%); iv) methyltriphenylphosphonium bromide, *n*-BuLi, THF, −10 to 25 °C, 4 h (88%); (v) cat. *p*TSA, MeOH, 25 °C, 24 h (83%); (vi) 2.5 equiv I_2, Na_2CO_3, AcCN, 1 h, 25 °C (37%); (vii) 3-bromophenol, K_2CO_3, AcCN, sealed-vial, 150 °C, 48 h (82%); (viii) bis(pinacolato)diboron, Pd(dppf)Cl_2·CH_2Cl_2, KOAc, DMF, 80 °C, 15 h (53%); (ix) **11**, $(Ph_3P)_4Pd$, Na_2CO_3, H_2O, DMF, 16 h, 80 °C (43%).

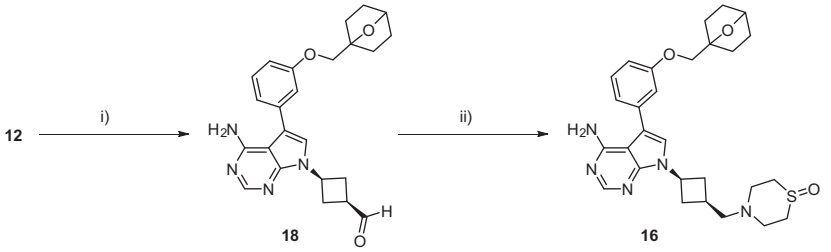

Scheme 4. Synthesis of the *cis*-methyl-(*N*-thiomorpholine sulfoxide) aminocyclobutyl analogue **16**. Reagents and conditions: (i) 2-iodoxybenzoic acid, AcCN, 1 h, 80 °C; (ii) thiomorpholine sulfoxide hydrochloride, $Na(OAc)_3BH$, $^iPr_2NEt$, CH_2Cl_2, 25 °C, 1 h, (2 steps 50%).

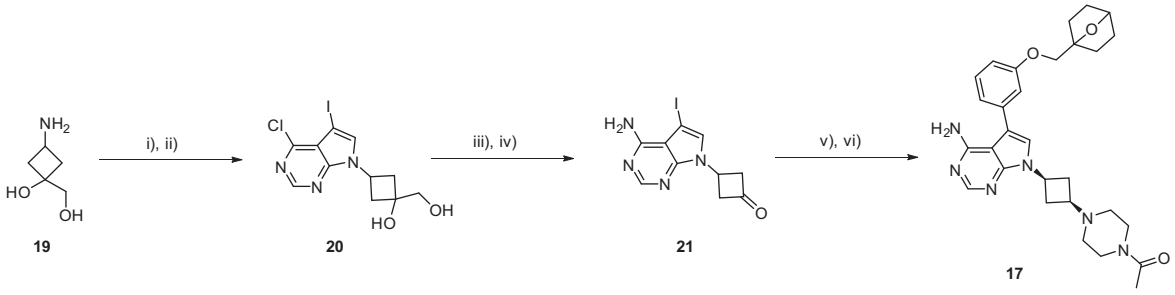

Scheme 5. Synthesis of the *cis*-(*N*-acylpiperazine) aminocyclobutyl analogue **17**. Reagents and conditions: (i) **8**, Hünig's base, EtOH, 4.5 h, reflux, then CF_3CO_2H, 1 h, reflux (91%); (ii) *N*-iodosuccinimide, DMF, 7 h, 60 °C (62%); (iii) NH_3, 1,4-dioxan, 15 h, 100 °C, sealed tube (71%); (iv) $NaIO_4$, THF/H_2O, 18 h, 25 °C (83%); (v) *N*-acetylpiperazine, $Na(OAc)_3BH$, AcOH, 1,2-DCE, 25 °C, 4 h (63%); (vi) **7**, $(PPh_3)_4Pd$, K_3PO_4, Na_2CO_3, DMF, H_2O, 3 h, 100 °C, then normal-phase separation of a 4:1 *cis*:*trans* isomer mixture (51%).

Table 2
Tertiary amine pK_a values and hERG-channel binding-affinities for NVP-AEW541 and the cyclic ether analogues **3**, **16** and **17**

Compound	pK_a	hERG IC_{50} (μM)
NVP-AEW541	9.5	0.13
3	n.d.	1.1
16	5.7	>30
17	5.9	15

With additional phenyl ether opportunities identified the attention turned to the pyrrolopyrimidine 7-substituent SAR interacting with the sugar-pocket region of the ATP-binding site. Extensive exploration of the series in this region identified two 3-cyclobutyl substituted variants which exhibited favourable profiles compared to NVP-AEW541 based upon: improved levels of IGF-1R activity and kinase selectivity; an adequate level of solubility with a tertiary amine of reduced pK_a, leading to lower levels of hERG activity; increased metabolic stability resulting in improved overall PK profiles. As a result these two pyrrolopyrimidine 7-substituents were extensively explored and are exemplified by the 7-oxabicyclo[2.2.1]heptan-1-ylmethylether analogues: methyl-(*N*-thiomorpholine sulfoxide) **16** (*cis*-CH_2-TMSO) and *cis*-4-(*N*-acetylpiperazine) **17** (*cis*-*N*-Ac-Pip). The routes to these two 3-cyclobutyl substituted analogues are exemplified as outlined below for the *cis*-CH_2-TMSO **16** in Scheme 4 and the *cis*-*N*-Ac-Pip **17** in Scheme 5.

Scheme 4 shows the synthesis of the *cis*-CH_2-TMSO analogue **16** starting from the *cis*-hydroxymethyl cyclobutyl analogue **12**: periodinane oxidation to the aldehyde **18** was followed by a reductive amination with thiomorpholine sulfoxide to give the desired compound **16**.

Scheme 5 shows the synthesis of the *cis*-*N*-Ac-Pip analogue **17**, starting from 3-hydroxy-3-hydroxymethylaminoazetidine **19**.[16] Cyclisation with 2-(4,6-dichloropyrimidin-5-yl)acetaldehyde **8** and iodination gave the pyrrolopyrimidine **20** which was reacted with ammonia, to displace the 4-chloro substituent, followed by oxidative cleavage of the diol to give the ketone **21**. Reductive amination of **21** with *N*-acetylpiperazine gave predominantly the *trans*-substituted cyclobutyl isomer which could be most readily separated from the *cis*-isomer following the Suzuki reaction with the boronate ester **7** to give the desired compound **17**.

Comparison of **16** and **17** with NVP-AEW541 and **3** showed comparable, or improved, IGF-1R activity, in particular for the

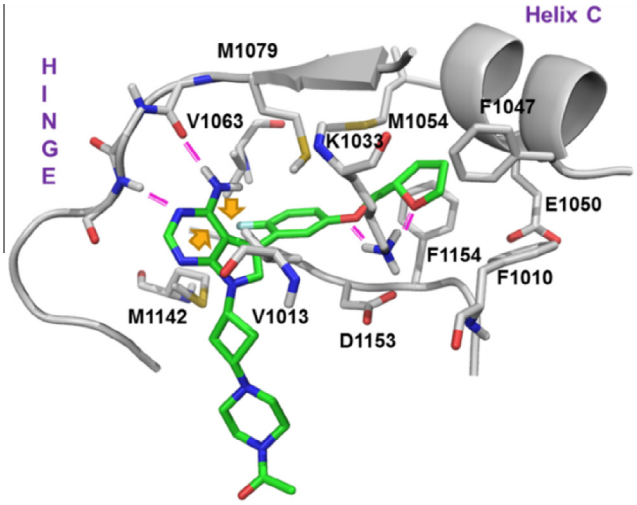

Figure 5. Model of compound **33** docked into the ATP site of IGF-1R. Hydrogen bonds are represented with magenta lines: pyrrolopyrimidine N5 to M1082 NH 3.2 Å, pyrrolopyrimidine 4-NH to E1080 C=O 3.0 Å, aryl ether to K1033 side-chain NH 3.1 Å, THF ether to K1033 side-chain NH 2.9 Å. Hydrophobic contacts between the 6-fluoro substituent and residues V1063 and M1142 are indicated by yellow arrows, van der Waals distances: M1142 to 6-fluorophenyl 3.4 Å, V1063 to 6-fluorophenyl 3.4 Å.

cis-*N*-Ac-Pip analogue **17**. Additionally, the lower pK_a values for both of the pyrrolopyrimidine 7-substituents were associated with decreased affinity for the hERG channel compared to the parent compounds, as shown in Table 2.[17]

To further explore the SAR of the series, molecular modelling indicated the potential for the introduction of fluorine into the 2- and 6-positions of the pyrrolopyrimidine 5-phenyl substituent to make additional favourable interactions within the ATP-pocket of IGF-1R. The incorporation of fluorine into the 2-position was anticipated to provide an additional hydrogen bond with Lys1033, and to make a hydrophobic contact with Val1013. The incorporation of fluorine into the 6-position was designed to create additional hydrophobic contacts with Met1142 and Val1063, and Figure 5 shows the 6-fluoro analogue **33** modelled into the ATP-pocket of IGF-1R highlighting these interactions. To fully explore the above possibility a fluorine scan was conducted across all four available positions within the pyrrolopyrimidine 5-phenyl substituent with the 7-oxabicyclo[2.2.1]heptan-1-ylmethylether and the 2-THF cyclic ethers combined with the optimal pyrrolopyrimidine 7-substituents, analogues **26**–**38** in Table 1. The fluorination of the linsitinib scaffold in the 2-position of the equivalent phenyl ring has also been shown to lead to improvements in activity, in particular increased residence time within the ATP-binding site of IGF-1R.[18]

To prepare the fluorinated analogues **26**–**38** the key boronate ester intermediates **22** were prepared as shown in Scheme 6. To begin the sequence the appropriately fluorinated 3-bromophenol derivatives **23** were either alkylated under Mitsunobu conditions to give the ether derivatives **24** which were then converted to the desired boronate ester intermediates. Alternatively, the fluorinated 7-oxabicyclo[2.2.1]heptan-1-ylmethylether boronate ester intermediates were prepared by the alkylation of the 3-bromophenols **23** with the iodide intermediate **6** in the first step, as outlined in Scheme 1. The boronate ester intermediates **22** were then coupled following the sequences shown in Schemes 2, 4 and 5 to prepare the analogues **26**–**38**, structures and IGF-1R data are shown in Table 1.

Consistent with the hypothesised impact of introducing fluorine into the 5-phenyl moiety, the 2- and 6-fluoro analogues exhibited comparable or slightly improved IGF-1R activities as exemplified by the *cis*-*N*-Ac-Pip analogues **27** and **32** compared to the unsubstituted compound **17**. The introduction of fluorine into the 5-position of the phenyl moiety led to a 4-fold decrease in IGF-1R activity, based upon a comparison between the *cis*-CH_2-TMSO analogues

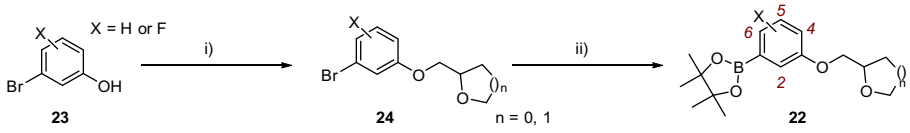

Scheme 6. Synthesis of the phenyl and fluorophenyl boronate ester 2-methyltetrahydrofuran ether and 2-methyloxetane ether building blocks **22** (X = H or F). Reagents and conditions: (i) diisopropyl azodicarboxylate, PPh_3, (*R*)- or (*S*)-(tetrahydrofuran-2-yl)methanol or (*R*,*S*)-(oxetan-2-yl)-methanol, THF, 24 h, 25 °C (58–82%); (ii) bis(pinacolato) diboron, 3 mol % $PdCl_2$(dppf), KOAc, DMF, 18 h, 100 °C (73–91%).

Table 3
Physicochemical and in vitro PK data for the 2-cyclic ether methyl ether analogues and the reference compounds NVP-AEW541 and linsitinib

Compound	*c*Log*P*/PSA (Å^2)	HDM FA (%)	Caco-2 A–B/B–A (10^{-6} cm s^{-1})	Rat microsome ER (%)	Rat PPB (%)
NVP-AEW541	4.4/72	99	5.4/10.1	74	95
Linsitinib	4.0/92	99	15.1/13.2	85	>99
1	3.0/81	86	n.d.	n.d.	n.d.
12	2.3/98	93	12.0/18.9	80	n.d.
13	2.8/98	99	n.d.	70	n.d.
16	2.3/98	26	4.4/21.2	72	85
17	2.0/101	49	5.6/15.5	61	89
25	2.0/98	30	n.d.	59	89
26	2.4/98	18	4.3/20.1	69	n.d.
27	2.1/101	40	n.d.	46	n.d.
28	1.7/101	24	n.d.	34	91
29	2.6/98	17	4.8/20.6	65	n.d.
30	2.3/98	22	2.9/17.8	76	n.d.
31	1.6/98	19	n.d.	20	n.d.
32	2.3/101	65	n.d.	46	n.d.
33	1.9/101	31	11.7/13.3	43	78
34	1.9/101	31	n.d.	46	n.d.
35	1.9/101	27	10.1/22.5	85	n.d.

PSA = polar surface area; HDM FA = hexadecane membrane permeability assay, predicting fraction absorbed from the gastrointestinal tract following oral dosing; PPB = plasma protein binding.[20]

Please cite this article in press as: Fairhurst, R. A.; et al. *Bioorg. Med. Chem. Lett.* (2016), http://dx.doi.org/10.1016/j.bmcl.2016.02.075

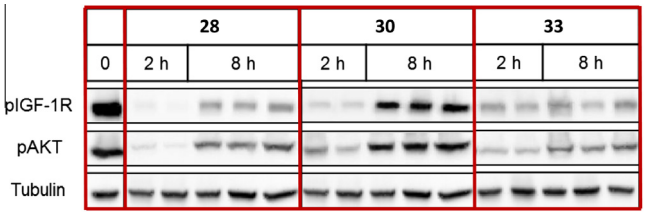

Figure 6. Extent of IGF-1R and AKT phosphorylation in NIH3T3:IFG-1R:IGF2 xenografts measured by Western blot analysis 2 and 8 h post treatment with compounds **28**, **30** and **33**.

Table 5
Biochemical and cellular InsR activities, and fold selectivities versus the IGF-1R for selected cyclic ether analogues, the phenol **2** and the reference compounds

Compound	IC_{50} (nM), (*IGF-1R fold selectivity*)		
	InsR	HEK	Ba/F3
NVP-AEW541	1018, (*17*)	892, (*14*)	244, (*12*)
Linsitinib	34, (*2.4*)	16, (*5.7*)	126, (*17*)
1	930, (*11*)	n.d.	64, (*5.3*)
2	3800, (*9.0*)	n.d.	638, (*2.1*)
3	510, (*11*)	471, (*8.9*)	65, (*4.6*)
28	94, (*5.9*)	102, (*6.4*)	36, (*2.4*)
33	175, (*15*)	166, (*13*)	93, (*5.8*)

36 and **25**. This decrease in activity with the 5-fluoro substituent was anticipated based upon a steric clash with the side chain of residue Val1063 in the modelled interaction. Introduction of fluorine into the 4-position proved to be more complex, and for the example **38** a comparable level of activity is retained compared to the non-fluorinated analogue **16**. However, a decrease in activity of 5-fold, or greater, was seen for other 4-fluoro analogues. Based upon the above observations, the further optimisation of the series was focused upon the 2- and 6-fluorinated analogues.

Exploring the series further, one trend that became apparent during the optimisation of the 2-cyclic ether methyl ethers was that higher levels of lipophilicity resulted in increased microsomal clearance values, and *c*log*P* values higher than 2.0 would likely be associated with high microsome extraction ratios (ER). Measured log*P* values were found to be in good agreement with the calculated values for the 2-cyclic ether methyl ether analogues. Physicochemical and in vitro PK parameters are shown for selected compounds in Table 3. Additionally, a reasonable in vitro/in vivo correlation was observed for the rat using microsomal clearance, at least to the extent that high in vitro microsomal clearance proved to be a very good predictor of unacceptably high in vivo clearance. For a number of the most interesting analogues the lipophilicity threshold for acceptable microsome clearance was often exceeded when comparing the [2.2.1]-bicyclic ether with the corresponding 2-THF ether analogues, for example comparing **16**, **27**, **29** and **32** with **25**, **28**, **30** and **33**. This increased metabolic stability for the 2-THF methyl ethers was sufficient to overcome the slightly lower levels of IGF-1R potency compared to the [2.2.1]-bicyclic ethers when considered in terms of the compounds overall profiles. Looking to further lower the level of lipophilicity the introduction of a 2-oxetanyl methyl ether was also investigated, as exemplified by compounds **31**, which led to a further increase in metabolic stability. However, the greater than 10-fold decrease in IGF-1R potency for the 2-oxetanyl methyl ethers was again observed and sufficient to concentrate the optimisation on the 2-THF and the [2.2.1]-bicyclic ethers.[9] Additionally, the nature of the cyclobutyl 3-substituent can also be seen to impact upon the metabolic stability, the higher lipophilicity of the *cis*-CH_2-TMSO analogues tending towards the highest levels of in vitro clearance for the analogues in Table 3.

A further key requirement for the optimisation of the series was to identify compounds with an adequate level of oral exposure to be able to deliver the targeted pharmacodynamic (PD) response at an acceptable dose level. Earlier PD/efficacy studies had established maintaining a trough inhibition of IGF-1R phosphorylation to be minimally required to deliver the maximum efficacy upon chronic dosing in a murine IGF-1R dependent human-xenograft model (NIH3T3:IFG-1R:IGF2).[19] Our goal was to achieve the maximum level of regression in the above model with a compound that could be administered twice-daily, ideally with a dose below 50 mg/kg, with a favourable prediction for translating the PK profile into man, and good overall drug properties.

Therefore, to further differentiate between the analogues of interest with high IGF-1R activities, and with higher levels of microsome stability: the extent of pathway inhibition following a single dose was assessed using the NIH3T3:IFG-1R:IGF2 xenograft model in the nude mouse. Compounds were administered orally as a single dose of 50 mg/kg and the extent of PD modulation was determined 2 h and 8 h after dosing. The PD response was assessed by western blot analysis to measure directly the level of IGF-1R phosphorylation, and further downstream in the pathway the level of AKT-phosphorylation was also measured. From this assessment, compounds **28** and **33** were identified as producing strong PD modulation at both time points, which was comparable to the reference compounds NVP-AEW541 and linsitinib when administered at an efficacious dose level, at the same time points. In contrast, a number of compounds only produced strong inhibition at the 2 h time point which was greatly diminished by the 8 h time point, as exemplified by compound **30**, data are shown in Figure 6.

From the above PD-modulation screening, the *cis*-*N*-Ac-Pip analogues **28** and **33** were identified for further profiling. Both compounds exhibited reasonable levels of solubility (>1 mM at pH 4.0 and >20 μM at pH 6.8) and rat PK studies showed both compounds were able to deliver high levels of exposure following oral dosing, data are shown in Table 4. In comparison to NVP-AEW541, in vivo clearance was greatly reduced, in line with the in vitro microsome data, leading to longer half-lives, even with significantly reduced volumes of distribution (Vss) and higher unbound fractions in plasma. Oral bioavailabilites (*F*) of 100% were determined for both **28** and **33**, when administered as suspensions, indicating good absorption from the gastro intestinal tract. This profile being consistent with the Caco-2 permeability data shown in Table 3, and highlighting the under prediction of the fraction absorbed by the passive membrane permeability assay for these two compounds.[20]

In addition, with the exception of the closely related InsR compounds **28** and **33** showed high levels of kinase selectivity against

Table 4
Rat PK data following iv and po dosing of compounds **28** and **33** compared to NVP-AEW541

Compound	Clearance (ml min^{-1} kg^{-1})	Vss (L/kg)	Terminal $t_{½}$ (h)	AUC po d.n. (nmol h L^{-1})	AUC iv d.n. (nmol h L^{-1})	Oral *F* (%)
NVP-AEW541	123 ± 13	19 ± 2.3	2.0 ± 0.5	311 ± 33	72 ± 13	23 ± 4
28	40 ± 12	6.5 ± 1.1	3.1 ± 1.8	862 ± 52	892 ± 285	97 ± 6
33	28 ± 5	5.0 ± 0.6	3.1 ± 2.4	1395 ± 193	1210 ± 184	115 ± 16

d.n. = dose normalised to 1.0 mg kg^{-1}.

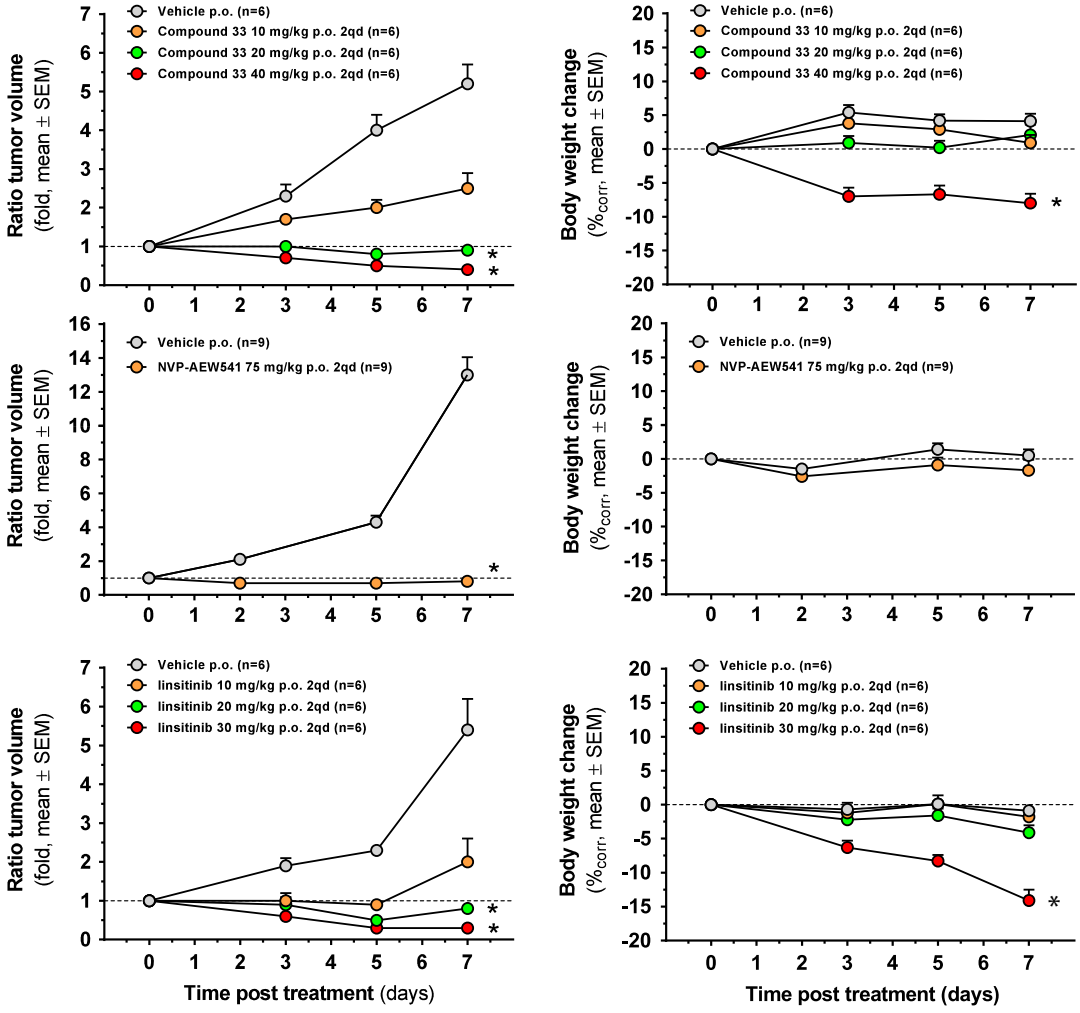

Figure 7. Efficacy study for compound **33**, NVP-AEW541 and linsitinib in nude mice bearing NIH3T3 xenotransplants.

an internal panel of sixty kinases.[12] Interestingly, and as previously reported for NVP-AEW541, some degree of selectivity versus the closely related InsR was observed for the 5-phenyl-4-aminopyrrolopyrimidine series, data are shown in Table 5. This trend was evident throughout the series, at both the biochemical and cellular level. To further explore this selectivity an in vivo comparison of the time course of IGF-1R PD modulation in the murine NIH3T3:IFG-1R:IGF2 tumour xenograft model compared to the inhibition of pInsR in the liver was conducted with compound **33**.[19] In line with the biochemical and cellular data this study also revealed evidence for a modest degree of selectivity in vivo between the IGF-1R and InsR receptors for this compound. However, the impact of any selectivity upon efficacy and tolerability remains unclear based upon the role IGF-1R/InsR hetero dimers may play in driving tumour growth.[2] Additional further off-target screening revealed both compounds **28** and **33** to have acceptable profiles, including affinities for the hERG channel >30 μM.[17]

Based upon their encouraging profiles, compounds **28** and **33** were investigated in efficacy studies using the NIH3T3:IGF-1R:IGF2 xenograft model in the nude mouse. From these studies **33** showed the most encouraging profile, and an extensive in vivo data set was generated for this compound and compared to NVP-AEW541 and linsitinib, key data are shown in Figure 7.[19] A clear anti-tumour dose response was observed for compound **33** when administered orally twice-daily at doses from 10 to 40 mg/kg for 1 week. When administered at a dose of 20 mg/kg compound **33** led to approximately tumour stasis (18% regression) and was well tolerated, as assessed by no change in body weigh compared to the vehicle treated control group. Similarly, stasis with an equivalent level of tolerability was also determined for NVP-AEW541 (19% regression) and linsitinib (16% regression) at doses of 75 and 20 mg/kg respectively. Increasing the doses of compound **33** and linsitinib to 40 and 30 mg/kg respectively led to comparable reductions in the tumour volumes (53% and 70% regression). However, this degree of response was associated with a reduction in body weight for both compounds, and represented the limit of tolerability in the mouse. As a further measure of tolerability, the functionality of the insulin pathway was assessed through an insulin-tolerance test (ITT) in the mouse for all three compounds. Comparing the ITT responses for compound **33** and linsitinib, the increases in circulating insulin and glucose levels supported these changes to be the key factor most likely driving the tolerability limitations of both compounds in this model.[21]

In conclusion, taking NVP-AEW541 as the starting point, the optimisation of a 5-phenyl-4-aminopyrrolopyrimidine series of IGF-1R inhibitors focused upon three areas: replacing the benzyl ether back-pocket binding moiety with a series of 2-cyclic ether methyl ethers; a fluorine scan of the 5-pheny group; and optimisation of the sugar-pocket binder. This approach resulted in the identification of compound **33** containing (*S*)-2-THF methyl ether 6-fluorophenyl ether back-pocket and *cis*-*N*-Ac-Pip sugar-pocket binding-moieties. Compared with NVP-AEW541, compound **33**

exhibited increased IGF-1R potency, reduced hERG activity and an improved PK profile. In a murine IGF-1R dependent xenograft model compound **33** inhibited tumour growth to the level of stasis at less than 30% of the dose required to produce the same effect with NVP-AEW541, and at the highest tolerated dose produced a comparable degree of tumour regression compared to linsitinib.

Acknowledgements

The authors would like to thank Peter Drueckes and Joerg Trappe for conducting biochemical assays; Markus Wartmann for conducting cellular assays; Rainer Aichholz, Francesca Blasco, Jerome Dayer, Francis Risser and Peter Wipfli for conducting pharmacokinetic studies; Rita Andraos-Rey for generating the NIH3T3:IGF-1R:IGF2 cell lines, Geneviève Albrecht for conducting in vitro and in vivo PD analyses; Jasmin Wirth, Milen Todorov and Mickael Le Douget for their excellent technical assistance.

Supplementary data

Supplementary data associated with this article can be found, in the online version, at http://dx.doi.org/10.1016/j.bmcl.2016.02.075.

References and notes

1. Pollak, M. *Nat. Rev. Cancer* **2008**, *8*, 925.
2. (a) Gallagher, E. J.; LeRoith, D. *Trends Endocrinol. Metab.* **2010**, *21*, 610; (b) Denley, A.; Wallace, J. C.; Cosgrove, L. J.; Forbes, B. E. *Horm. Metab. Res.* **2003**, *35*, 778.
3. Arteaga, C. L.; Kitten, L. J.; Coronado, E. B.; Jacobs, S.; Kull, F. C.; Allred, D. C.; Osborne, C. K. *J. Clin. Invest.* **1989**, *84*, 1418.
4. Pollak, M. *Nat. Rev. Cancer* **2012**, *12*, 159.
5. (a) Negi, A.; Ramarao, P.; Kumar, R. *Mini-Rev. Med. Chem.* **2013**, *13*, 653; (b) Sarma, P. K. S.; Tandon, R.; Gupta, P.; Dastidar, S. G.; Ray, A.; Das, B.; Cliffe, I. A. *Expert Opin. Ther. Patents* **2007**, *17*, 25.
6. (a) Puzanov, I.; Lindasy, C. R.; Goff, L.; Sosman, J.; Gilbert, J.; Berlin, J.; Poondru, S.; Simantov, R.; Gedrich, R.; Stephens, A.; Chan, E.; Ecans, T. R. J. *Clin. Cancer Res.* **2015**, *21*, 701; (b) Mulvihill, M. J.; Buck, E. The Discovery of OSI-906, a Small-Molecule Inhibitor of the Insulin-Like Growth Factor-1 and Insulin Receptors. In *Accounts in Drug Discovery: Case Studies in Medicinal Chemistry*; Barrish, J. C., Carter, P. H., Cheng, P. T. W., Zahler, R., Eds.; Drug Discovery Series No. 4; Royal Society of Chemistry, 2011.
7. Garcia-Echeverria, C.; Pearson, M. A.; Marti, A.; Meyer, T.; Mestan, J.; Zimmermann, J.; Gao, J.; Brueggen, J.; Capraro, H.-G.; Cozens, R.; Evans, D. B.; Fabbro, D.; Furet, P.; Graus Porta, D.; Liebetanz, J.; Martiny-Baron, G.; Ruetz, S.; Hofmann, F. *Cancer Cell* **2004**, *5*, 231.
8. (a) Weisberg, E.; Nonami, A.; Chen, Z.; Nelson, E.; Chen, Y.; Liu, F.; Cho, H. Y.; Zhang, J.; Sattler, M.; Mitsiades, C.; Wong, K.-K.; Liu, Q.; Gray, N. S.; Griffin, J. D. *Clin. Cancer Res.* **2014**, *20*, 5483; (b) Suda, K.; Mizuuchi, H.; Sato, K.; Takemoto, T.; Iwasaki, T.; Mitsudomi, T. *Int. J. Cancer* **2014**, *135*, 1002; (c) Ioannou, N.; Seddon, A. M.; Dalgleish, A.; Mackintosh, D.; Modjthedi, H. *BMC Cancer* **2013**, *13*, 41.
9. Stauffer, F.; Jacob, S.; Scheufler, C.; Furet, P. *Bioorg. Med. Chem. Lett.* **2016**, *26*. http://dx.doi.org/10.1016/j.bmcl.2016.02.074.
10. In vitro and in vivo metabolism data for NVP-AEW541 and representative 2-cyclic ether methylether derivatives are included in Supplementary data.
11. Widler, L.; Green, J.; Missbach, M.; Šuša, M.; Altmann, E. *Bioorg. Med. Chem. Lett.* **2001**, *11*, 849.
12. Kinase selectivity was assessed against a panel of biochemical assays: data for compounds NVP-AEW541, **1**, **2**, **3**, **28** and **33** are included in Supplementary data.
13. (a) Experimental details of the syntheses of the final products and intermediates are described. In: Chen, B.; Fairhurst, R. A.; Jiang, S.; Lu, W.; Marsilje, T. H.; McCarthy, C.; Michellys, P-Y.; Stutz, S. WO 2012/120469, Sep 13, 2012.; (b) Chen, B.; Fairhurst, R. A.; Floersheimer, A.; Furet, P.; Guagnano, V.; Jiang, S.; Lu, W.; Marsilje, T. H.; McCarthy, C.; Michellys, P-Y.; Stauffer, F.; Stutz, S.; Vaupel, A. WO2011/029915, Mar 17, 2011.
14. Slade, J.; Bajwa, J.; Liu, H.; Parker, D.; Vivelo, J.; Chen, G.-P.; Calienni, J.; Villhauer, E.; Prasad, K.; Repic, O.; Blacklock, T. J. *Org. Process Res. Dev.* **2007**, *11*, 825.
15. Details of the biochemical IGF-1R and InsR, and the cellular HEK and Ba/F3 assays are described in Supplementary data.
16. Jandu, K. S.; Barrett, V.; Brockwell, M.; Cambridge, D.; Farrant, D. R.; Foster, C.; Giles, H.; Glen, R. C.; Hill, A. P.; Hobbs, H.; Honey, A.; Martin, G. R.; Salmon, J.; Smith, D.; Woollard, P.; Selwood, D. L. *J. Med. Chem.* **2001**, *44*, 681.
17. Details of the hERG-channel binding assay are described in Supplementary data.
18. Jin, M.; Petronella, B. A.; Cooke, A.; Kadalbajoo, M.; Siu, K. W.; Kleinberg, A.; May, E. W.; Gokhale, P. C.; Schulz, R.; Kahler, J.; Bittner, M. A.; Foreman, K.; Pachter, J. A.; Wild, R.; Epstein, D.; Mulvihill, M. J. *Med. Chem. Let.* **2013**, *4*, 627.
19. Details of the NIH3T3:IGF-1R:IGF2 xenograft model, including the comparison of IGF-1R and InsR PD modulation for compound **33**, are described in Supplementary data.
20. Details of the in vitro permeability assays and plasma protein binding measurements are described in Supplementary data.
21. Details of the insulin-tolerance test are described in Supplementary data.